Environmental and
Biogeochemical Processes

Original Research

Open Access

https://doi.org/10.48130/ebp-0025-0006

A bio-photovoltage soil-microbe battery for antibiotic degradation in the dark

Shunling Li[1,2], Ye Chen[1,2], Min Wu[1,2,3], Peng Zhang[1,2], Peng Cui[1,2], Wenyan Duan[1,2], Bo Pan[1,2*] and Baoshan Xing[3*]

Received: 1 July 2025

Revised: 6 August 2025

Accepted: 22 August 2025

Published online: 15 September 2025

Abstract

Solar energy sustains biogeochemical functions in soils. However, its utilization in saturated subsurface zones remains constrained by limited light penetration. In this study, it was revealed that iron mineral-*Bacillus megaterium* (*B. megaterium*) biofilms function as geochemical capacitors, wherein a redox pseudo-capacitance enables photon-to-electron conversion and dark-phase electron release for contaminant degradation. Fe_2O_3/*B. megaterium* composite at a 1:2 mass ratio reached a total accumulated charge ($\Sigma\sigma$) of 8.06 μC·cm^{-2} during light-dark cycles, with net charge increasing from 2.87 to 4.08 μC·cm^{-2}. Electrochemical analysis indicated that capacitance exclusively forms at mineral-microbial interfaces, but not in single-component systems. A higher microbial density corresponded to increased $\sum\sigma$ and Fe(II) contents, demonstrating that the biofilm enhances the Fe(II)/Fe(III) cycle for the capture and storage of photo-generated charges. Notably, 60 min illumination resulted in a significant degradation in dark phase for tetracycline hydrochloride (20%) and chloramphenicol (22%), outperforming the systems subjected to 20 min illumination by 46.7%–66.7%. The interactions between iron minerals and bacteria formed a biofilm acting as a 'biocapacitor', wherein Fe(II)/Fe(III) cycle, coupled with bacteria, establishes a redox relay system, channeling stored electrons toward pollutants.

Keywords: Bio-photovoltage, *Bacillus megaterium*, Fe_2O_3, Antibiotic degradation, Iron minerals, FeOOH

Highlights

- A bio-photovoltage soil-microbe battery for antibiotic degradation in the dark is proposed.
- Iron mineral–*B. megaterium* biofilms function as geochemical capacitors, enabling photon-to-electron conversion, charge storage, and controlled release for antibiotic degradation.
- Fe_2O_3/*B. megaterium* achieves 8.06 μC·cm^{-2} charge storage via interfacial capacitance absent in single-component systems.
- Sixty-min illumination enables 20%–22% antibiotic degradation in dark phase, outperforming 20-min treatment by 47%–67%.
- Mineral–bacterial interface forms a redox relay system, channeling stored electrons for contaminant degradation.

* Correspondence: Bo Pan (panbocai@aliyun.com); Baoshan Xing (bx@umass.edu)
Full list of author information is available at the end of the article.

Graphical abstract

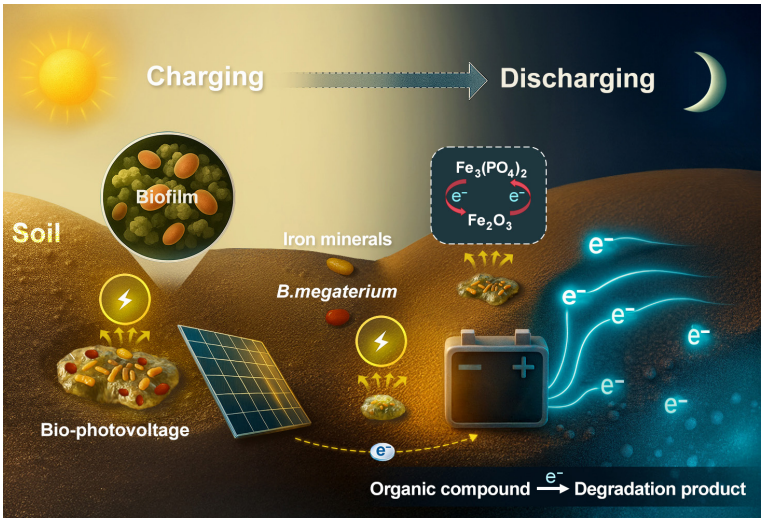

Introduction

Solar radiation is the main energy source for the surface ecosystem, and it is the original driving force for the ecosystem to maintain its normal operation and development[1]. The energy captured by plant photosynthesis is recognized as the main driver for the formation of organic matter utilized by soil microorganisms, particularly when the vadose zone is unsaturated[2]. In contrast to the conventional biophotoelectrochemistry in phytoplankton through photosynthesis, recent studies suggested that non-phototrophic microorganisms in soils and sediments are able to harvest extracellular electrons, including the photoexcited electrons from photosensitizers, such as minerals and photosynthetic bacteria[3,4]. This discovery suggested that solar energy may have a more extensive impact on microbial metabolism and geochemical processes, even in saturated soils and sediments.

This emerging field of biophotoelectrochemistry leverages live microbial biofilms to harness sunlight for electricity generation[5], potentially channeling photoexcited electrons into the opaque zones of soil. The 'mineral films' formed through the interaction of semiconductor minerals such as Fe, Cu, Mn, or Ti minerals and microorganisms can absorb sunlight and promote the growth of chemosynthetic autotrophic microorganisms, which have been discovered in three distinct habitats in China, including the rock paintings of the northwest Gobi Desert, the karst landforms in the southwest, and the red soil in the south[3]. These discoveries suggest mineral-microbial biofilms may extend electron transport chains beyond conventional limits, enabling novel energy cascades in dark environments. This generally overlooked process may have played critical roles in biogeochemical functions such as contaminant mitigation in soils and sediments via photoelectron-driven redox reactions. Notably, transient photocurrents in abiotic systems decay within milliseconds, preventing energy utilization beyond the photic zone. While recent studies confirm non-phototrophic microbes harvest photoelectrons from mineral photosensitizers[6–8], the mechanistic linkage between photoelectron transfer and microbial energy utilization remains unresolved. Specifically, how do biofilms convert ephemeral photoelectrons into persistent metabolic energy for dark-phase biogeochemical processes?

Bacillus is a group of bacteria with high abundance in soil. *Bacillus megaterium* (*B. megaterium*) has been demonstrated to be electrochemically active. This study employed hematite (Fe_2O_3) and goethite (FeOOH) as the model minerals and *B. megaterium* as the model microbe to explore the transfer and utilization of photoelectrons following the interaction between bacteria and iron minerals. Our primary focus is on the accumulation, storage, and release of electrons during light-dark cycles following the interaction between *B. megaterium* and iron minerals, as well as the subsequent effects on organic compound degradation in the dark. This line of study not only sheds light on biogeochemical processes but also explores sustainable techniques to mediate pollution control.

Materials and methods

B. megaterium and iron oxide mineral cultivation experiments

The *B. megaterium* strain was isolated from soil (Kunming, China)[9]. The 16S rDNA sequences were analyzed using the National Center for Biotechnology Information database, GenBank. The culture methods for *B. megaterium* cells are detailed in previous literature[9]. *B. megaterium* cells were obtained by centrifugation at 6,577 × g for 15 min at 4 °C, followed by freeze-drying. Various proportions of *B. megaterium* cells and Fe_2O_3 were dispersed in sterile distilled water for 1 d at 30 °C with shaking at 150 rpm in a constant temperature shaker, centrifuged at 8,000 × g, and washed 10 times with distilled water. The obtained Fe_2O_3–*B. megaterium* composites were freeze-dried separately for further use.

Photoelectrochemical testing

Three different types of electrodes, based on a saturated calomel electrode, indium-tin oxide, or a platinum wire, were used. The photoelectrodes were prepared by the drop-coating method[10]. Six mg of the composites were dispersed with 600 μL 30% ethanol, 100 μL 3.75% acetic acid, and 50 μL Nafion, and the mixture was sonicated for 1 h[11]. Acetic acid serves as a multifunctional additive that stabilizes dispersion through protonation-induced electrostatic repulsion, enhances charge transfer via proton-coupled redox mediation, and controls film morphology by modulating solvent evaporation dynamics[12]. The electrodes were then coated with 200 μL of the mixture to form a thin film. Subsequently, the sample solution was loaded onto the conductive surface of indium-tin oxide conductive glass with a physical area of 1 cm^2 and dried at room temperature for

12 h to form a thin film. Open circuit potential-time (OCPT), Electrochemical impedence spectroscopy (EIS), Amperometric i-t curve (i-t curve), and Tafel analysis were performed.

Analysis of physicochemical properties and electronic structure of composites

The morphologies of the composites were analyzed using field emission scanning electron microscopy (Hitachi Regulus 8,100, Zeiss Sigma 300). The composition of surface elements was analyzed using energy-dispersive X-ray spectroscopy (X-Max N, Oxford Instruments). The X-ray diffraction (XRD) patterns were recorded in the range of 5°–80° at 40 kV and 30 mA to determine any changes in the crystal structure of the minerals. The chemical composition of the samples was characterized by a Fourier transform infrared spectrophotometer (Nicolet iS50, Thermo). Additionally, the Raman spectra were obtained using a Raman microscope (Renishaw inVia, USA) equipped with a 532 nm laser.

B. megaterium activity

The investigated particles were dispersed into sterile distilled water and cultured on Luria-Bertani agar plates[9]. The dead and live conditions of bacteria in the investigated systems were characterized by a confocal laser scanning microscope (Zeiss LSM880) using the LIVE/DEAD BacLight viability stain kit from Molecular Probes (Eugene, OR, USA). *B. megaterium* biofilms were imaged on an Olympus Fluoview FV3000 confocal microscope (Olympus, Japan).

Light-induced degradation of antibiotics

This study investigated the transformation of chloramphenicol (CPL) and tetracycline hydrochloride (TCH) by Fe_2O_3/*B. megaterium* or FeOOH/*B. megaterium*. Degradation of these antibiotics in Fe_2O_3/*B. megaterium* or FeOOH/*B. megaterium* was investigated under dark conditions after exposure to sunlight for 0, 20, and 60 min.

Antibiotics in solid and liquid phase after reaction were evaluated by HPLC (Agilent 1,260 Infinity II HPLC equipped with a C18 column) at 30 °C. CPL was measured by a fluorescence detector at an excitation wavelength of 278 nm; the mobile phase was methanol/water (60:40, v/v) at a flow rate of 1 mL·min^{-1}[13]. For TCH, the detection conditions were as follows: the mobile phase comprised acetonitrile and ultrapure water in a ratio of 35:65, with a detection wavelength of 280 nm, a flow rate of 1.0 mL·min^{-1}, an injection volume of 10 μL, and a column temperature also maintained at 30 °C[14]. The retention time for TCH was approximately 3.4 min.

Statistics and reproducibility

All data are presented as mean ± standard deviation (SD), and statistical analyses and graphs were performed using GraphPad Prism 10.0.2. Significant differences were determined by Duncan's multiple range test at $p < 0.05$. One-way analysis of variance (ANOVA) was used to assess the data (means ± SD, n = 3) using IBM SPSS statistics 20.0.

Results and discussion

Bacteria-iron minerals co-culturing exhibits charge-discharge function and photovoltage memory effect

The accumulation and release of electrons during light-dark alternation was investigated in co-cultures of *B. megaterium* and Fe_2O_3 or FeOOH. The morphology and structure of iron mineral surfaces were altered by *B. megaterium*. For example, a multiphase structure characterized primarily by flake-like and granular morphologies was observed after co-culturing with Fe_2O_3 (Fig. 1a–d), and the bacteria remained active (Supplementary Fig. S1). Interestingly, this co-cultured system exhibited distinctive continuous charge-discharge characteristics under light-dark alterations. As the number of light-dark cycles increased, the photocurrent density gradually rose, while the dark current density consistently decreased (Supplementary Fig. S2). A denser biofilm (i.e., a higher ratio of bacterial content) corresponded to a greater photocurrent density (Supplementary Fig. S2). The difference between charge accumulations (σ) induced in light and released in dark showed fewer variations in pure Fe_2O_3 or *B. megaterium* systems compared to the co-culturing systems (Fig. 1e). After three cycles, their total accumulated charge ($\sum\sigma$) approximately equaled the overall released charge (Fig. 1f). However, the σ values of the co-culturing systems under illuminated conditions consistently exceeded those released in dark, and this disparity gradually increased with the number of cycles. Consequently, the $\sum\sigma$ values of the co-culturing system in light were significantly higher than those released in the dark ($p < 0.001$). Notably, more microbial biomass corresponded to a higher $\sum\sigma$, indicating that a dense biofilm may be more conducive to capturing and storing photo-generated charges. It should be noted that some electrons that were not fully released during the dark period became 'residual charge' accumulated in the system. The net accumulated charge increased from 2.87 to 4.08 μC·cm^{-2} ($p < 0.001$). Comparative analysis of adjacent mixing ratios (2:1 vs 1:1; 1:1 vs 1:2) revealed no statistically significant differences in $\sum\sigma$ values ($p > 0.05$). However, with extended cultivation, the system developed well-defined lamellar architectures under the 1:1 ratio condition (Supplementary Fig. S3). These structurally optimized biofilms showed a 3.2-fold increase in net charge accumulation, from 3.98 to 12.60 μC·cm^{-2} ($p < 0.0001$; Supplementary Fig. S3). These findings highlighted the critical role of bacteria in regulating the optoelectronic storage performance of the co-cultured systems.

The Fe_2O_3/*B. megaterium* biofilm demonstrated a photovoltaic effect according to OCPT results, which increased with the proportion of bacteria (Fig. 1g). However, the photoelectric conversion mechanism of this biofilm differs from that of the traditional photoelectric effect. When shifting from dark to light exposure, all the investigated systems demonstrated photovoltaic effects. The photovoltage (V_{oc}) of *B. megaterium* reached −69 mV, surpassing the −18 mV observed for Fe_2O_3. The V_{oc} values in the co-culturing systems increased from −43 to −62 mV with the increased bacterial concentration (Fig. 1g). The E_{OCP} of co-culturing systems shifted to more negative values with increased bacterial concentration under light exposure, but to more positive values in the dark. This phenomenon probably indicated that co-culturing was a photo-regenerative electronic capacitor: The compact biofilm enhances the electron storage and conversion capacity, achieving efficient photonic energy conversion and slow release. Notably, the E_{OCP} of the biofilm always recovered after the light was turned off, suggesting that this co-culturing system possesses a photoelectric memory function (Supplementary Fig. S4).

In general, these results indicate that the biofilm formed through the interaction of Fe_2O_3 and *B. megaterium* exhibited a capability of continuous photo-charging. This charging process was enhanced with light-dark cycles and the proportion of bacteria in the co-culture system. The interaction between FeOOH and *B. megaterium* followed a similar pattern (Supplementary Figs S5–S7). These findings may provide new insights into carbon and nitrogen cycles in soil, as well as strategies for pollution control. Therefore, we propose the following hypothesis: photoelectrons stored during light radiation at the iron-microbe biofilm can facilitate the transformation of pollutants in soil and even groundwater.

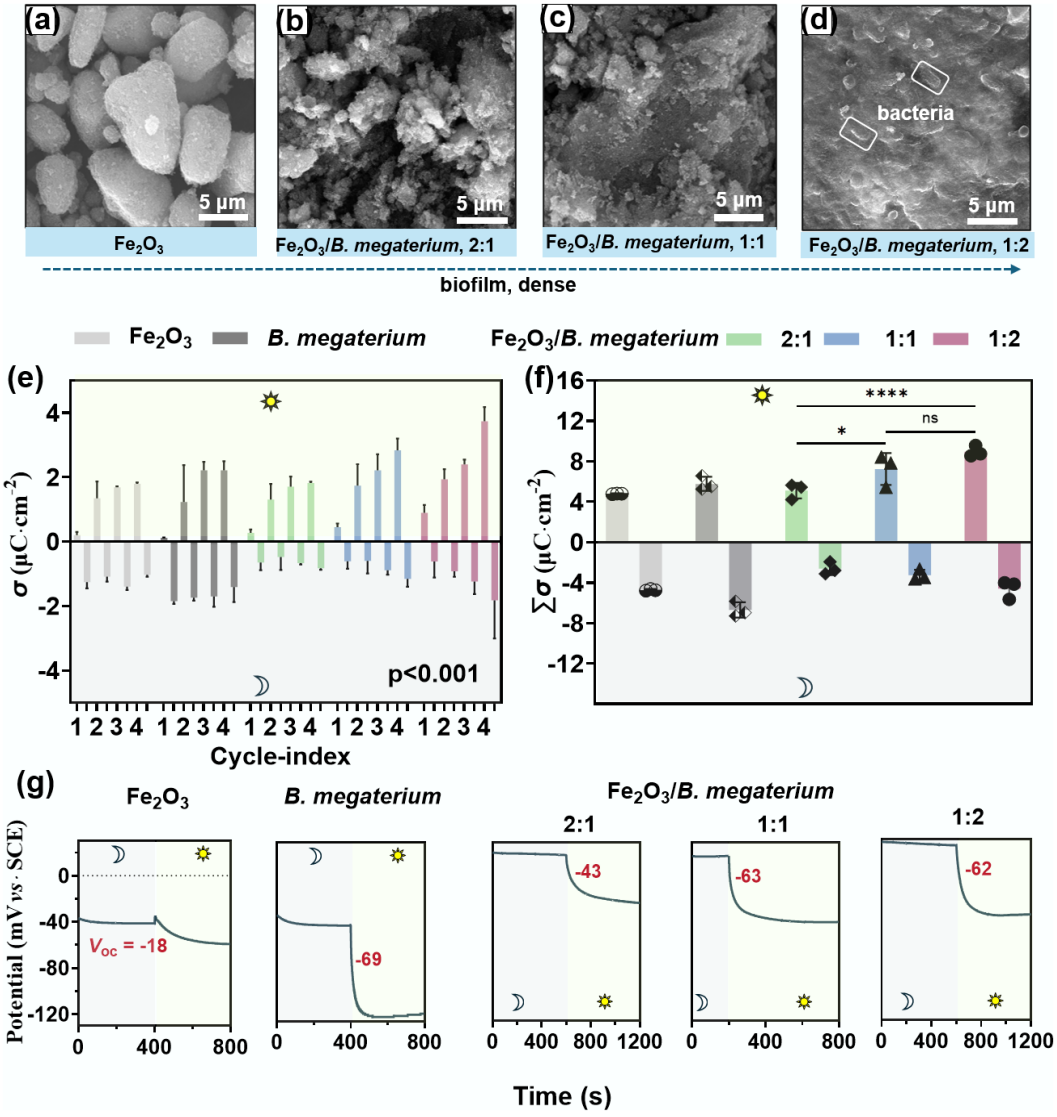

Fig. 1 The biofilms formed in Fe_2O_3–*B. megaterium* systems showed photovoltaic effects. (**a**)–(**d**) The surface morphologies of the biofilm on Fe_2O_3 displaying a lamellar structure. (**e**) This Fe_2O_3-*B. megaterium* system showed electro-charging and discharging processes under alternating light and dark conditions ($p < 0.001$). (**f**) The summarized $\sum\sigma$ values of the co-culturing system in light were significantly higher than those released in dark. (**g**) This biofilm exhibited a photovoltaic effect in dark-light cycles. The interaction between FeOOH and *B. megaterium* followed a similar pattern as presented in Supplementary Figs S5–S7.

Organic degradation in the dark after photo-charging of the composites

Iron mineral-bacterial biofilms exhibit photon memory, distinguishing them from single-component systems. The Fe_2O_3/*B. megaterium* composite system demonstrated minimal degradation of TCH and CPL under continuous darkness (light exposure of 0 min). In the following experiment, the Fe_2O_3/*B. megaterium* composite was subjected to continuous light for 20 min. Then the light was turned off, and pollutants were introduced. The degradation efficiency of TCH reached 12% within the first 20 min of the reaction, while CPL degradation was 15% at 20 min (Fig. 2a). When the light illumination was extended to 60 min, the following degradation efficiencies in dark reached up to 20% (TCH), and 22% (CPL), representing significant enhancements of 66.7% and 46.7%, respectively (Fig. 2a). However, the separated systems of Fe_2O_3 or *B. megaterium* showed negligible degradation after both 20 min and 60 min of light exposure. These results indicated that the Fe_2O_3/*B. megaterium* co-culturing systems can degrade antibiotics in the dark after being charged in light. Again, the FeOOH-based system demonstrated a similar trend (Fig. 2b). These photonic memory properties of iron mineral/bacterial composites could degrade organic pollutants, which may play a significant role in their environmental behavior.

Conversion of iron minerals in the co-culturing systems

To elucidate the degradation mechanism of organic pollutants in bacteria-iron mineral systems, the photoelectrical response, interfacial architecture, and compositional evolution of the biofilm were investigated. Elemental mapping revealed a homogeneous distribution of Fe, O, C, N, P, and S across the biofilm surface, with C, N, P, and S originating from bacterial incorporation (Supplementary Figs S8 and S9). The enhanced electrochemical activity of the iron mineral/*B. megaterium* could be attributed to the incorporation of these biological elements. High-resolution XPS spectra of the Fe2p orbitals

displayed a negative shift in the binding energies of Fe(III) at 710.8 and 723.5 eV following interaction with *B. megaterium*[15] (Fig. 3a). Notably, two new peaks emerged at 708.9 eV ($2p_{3/2}$) and 721.7 eV ($2p_{1/2}$), representing Fe(II) species[16] (Fig. 3a). The Fe(II) content increased from 17.4% to 28.4% with a rise in the initial proportions of *B. megaterium* (Fig. 3a and Supplementary Fig. S8), confirming microbial-driven reduction of Fe_2O_3. The peaks for PO_4^{2-} (131.86 eV), Fe–N (398 eV)[17], pyridinic-N/amino-N (399 eV), and C–N (273.5 eV) were observed in the biofilm[16] (Supplementary Fig. S9). These results demonstrate that *B. megaterium* was able to reduce Fe_2O_3 while introducing C, N, P, O, and S in the system, forming $Fe_3(PO_4)_2$ and modulating its electronic and chemical properties to favor antibiotic degradation.

XRD analysis also revealed weakened diffraction peaks and the emergence of new $Fe_3(PO_4)_2$ peaks at 20°, 38°, and 54° in the co-culturing systems[18,19] (Fig. 3b), confirming Fe(III) reduction, which was consistent with XPS results. Fe(II) content increased up to 41.3% over time (Supplementary Fig. S10). The mixed Fe(II)/Fe(III) in Fe_2O_3/*B. megaterium* biofilm enabled photoelectron storage, as evidenced by their stronger Raman peaks over Fe_2O_3-only systems (Fig. 3c). *B. megaterium* also reduced Fe(III) in FeOOH to Fe(II) as presented in Supplementary Figs S11–S13. In general, metabolic products such as pyridinic-N, amino-N, and PO_4^{3-} could reduce charge-transfer resistance. The co-culturing systems synergistically enhanced charge storage, carrier separation, and interfacial electron transfer, which were critical for redox-driven degradation.

Electrochemical characterization of the co-culturing systems

The electron storage, transfer, and release are determined by the resistance *R* and capacitance, which can be reliably analyzed using EIS under an open circuit voltage[20]. The phase angle Bode plot was employed to assess the number of interfacial electrochemical processes involved in EIS. For individual systems of Fe_2O_3 and *B. megaterium*, a peak in the middle-low frequency (MF-LF) region was observed (Supplementary Figs S14 and S15), indicating the presence of one-time constant τ. In comparison, the Bode plot of Fe_2O_3/*B. megaterium* composites showed one peak in the MF-HF region and two troughs, corresponding to two time constants. The maximum phase angle of Fe_2O_3/*B. megaterium* systems (52.6°–55.4°) was lower than those of Fe_2O_3 or *B. megaterium* (Supplementary Fig. S14), suggesting the enhanced charge transfer in the composites. The slopes of Bode modulus plots for the investigated composites are close to −1 in MF-HF region (Supplementary Fig. S14), indicating a typical capacitive behavior[21]. The τ values of Fe_2O_3/*B. megaterium* composites were 2–3 magnitudes lower than that of the individual components of Fe_2O_3 or *B. megaterium* (Fig. 4a), indicating that the interaction between bacteria and iron minerals significantly enhanced the migration rate of photogenerated charge carriers (electron-hole pairs). *B. megaterium* forms coordination bonds with the Fe_2O_3 surface through functional groups such as carboxyl and amino groups, creating efficient electron transfer pathways[22,23], which suppresses carrier recombination and accelerates their migration to the electrode interface.

The electrochemical processes were conceptualized using the equivalent electric circuit model (Supplementary Table S1). The interfacial capacitance (Q_1) increased by 5–9 times and was accompanied by the formation of a series capacitance (Q_2) (Fig. 4b and Supplementary Table S1). The electron transfer resistance (R_{ct}) of Fe_2O_3/*B. megaterium* composites were reduced by about three orders of magnitude compared to Fe_2O_3 or *B. megaterium* alone (Fig. 4c). These results suggested that the bacteria-mineral interface forms a pseudocapacitive structure, promoting charge separation and storage through interfacial polarization effects. The Tafel curve further revealed that the exchange current density (*j*) of the biofilm reaches up to 5.7×10^3 A·cm^{-2}, which was six orders of magnitude higher than that of a single component, indicating that the heterojunction significantly reduced the charge transfer energy barrier and optimized the kinetics of redox reactions (Fig. 4d and Supplementary Fig. S16).

These comprehensive descriptions indicate that Fe_2O_3 and *B. megaterium* interact to form a large 'biological capacitor', which can buffer transient photonic current fluctuations, enhance photoelectric conversion efficiency, and enable pollutant degradation in the dark after light charging. The photocurrent response of the Fe_2O_3/*B. megaterium* biofilm exhibits a unique stepwise growth characteristic, achieving the dark-state degradation of TCH and PCL after light charging. This phenomenon may be attributed to: (1) the synergistic effect of the Fe(II)/Fe(III) redox pair on the surface of Fe_2O_3 and

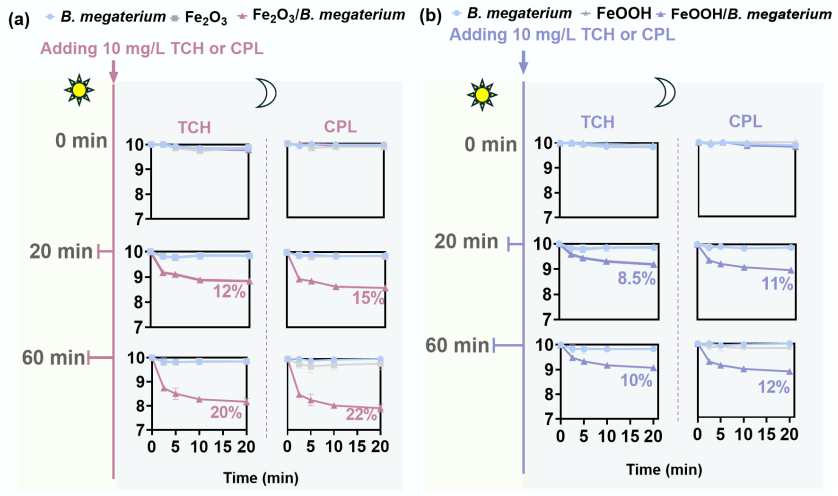

Fig. 2 Prolonging the illumination duration of the iron mineral/*B. megaterium* co-culturing systems enhances both the rate and extent of antibiotics degradation. When TCH or CPL was introduced to the systems after being illuminated for 0, 20, and 60 min, (**a**) the Fe_2O_3/*B. megaterium*, and (**b**) FeOOH/*B. megaterium* co-culturing systems promoted pollutant degradation of TCH or CPL in a dark environment. Notably, the degradation of antibiotics by the biofilm formed through biofilm was independent of free radicals (Supplementary Text 1).

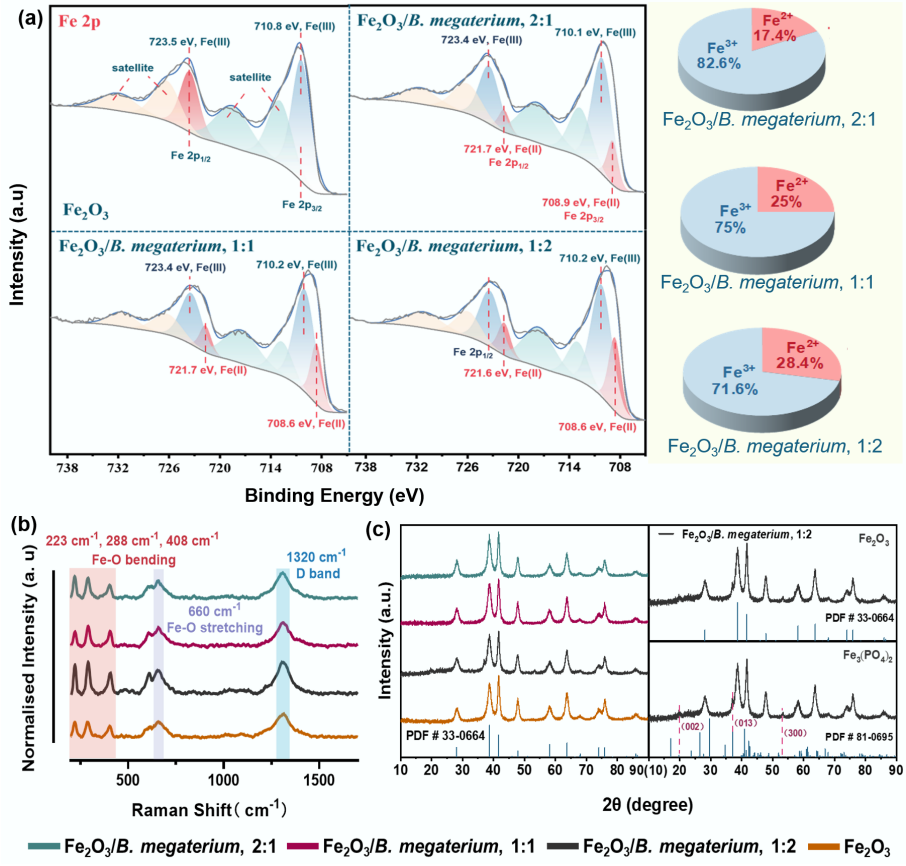

Fig. 3 *B. megaterium* reduces the Fe(III) in Fe_2O_3 to $Fe_3(PO_4)_2$, along with the altered elemental composition and electronic structure of the mineral. The content of Fe(II) increased with the increase of (**a**) bacteria proportion, (**b**) crystal type, and (**c**) Raman intensity also changed after *B. megaterium* and Fe_2O_3 co-culturing.

microbial electron shuttles forming a distributed charge storage network; (2) the biologically mediated transmembrane transfer of the stored electrons to sustain pollutant degradation; (3) the smooth photocurrent buffered by capacitive effects to ensure operational stability.

The sustained pollutant degradation of the light-activated composites in the dark suggests effective trapping and storage of photogenerated electrons. Bacterial metabolites from *B. megaterium*, such as extracellular polysaccharides and electron shuttles, synergistically formed a 'biological capacitor' with hydroxylated iron mineral surfaces, facilitating the transmission of stored electrons to pollutant molecules.

Conclusions

The iron-metabolizing bacterium *B. megaterium* is widely distributed in terrestrial and aquatic ecosystems, particularly in plant rhizospheres (colonizing at 10^5–10^7 CFU·g^{-1} on crops like rice and alfalfa) and tidal sediments, where it frequently interfaces with iron oxides. Through controlled experiments mimicking natural iron-rich environments, we observed bio-photovoltage memory in Fe_2O_3/*B. megaterium* systems. The composite at a 1:2 mass ratio reached $\sum\sigma$ of 8.06 μC·cm^{-2}, with the net charge increasing from 2.87 to 4.08 μC cm^{-2}. A higher microbial density corresponds to an increased $\sum\sigma$ and Fe(II) content, suggesting that a dense biofilm enhances Fe(II)-mediated processes, which facilitate the capture and storage of photo-generated charges. We propose that after the light is turned off, the enriched photogenerated electrons are released in the dark, generating a photovoltaic effect that drives pollutant degradation. This biofilm demonstrates sustained electron storage and release capability without continuous illumination, as evidenced by continued degradation of TCH and CPL for 1 h in the dark post-illumination. Notably, extended charging time enhances both the rate and extent of TCH and CPL degradation under dark conditions. These results provide new insights into the treatment of soil, sediment, and groundwater pollutants, and contribute to our understanding of element cycling and pollutant degradation in soil and sediment.

Supplementary information

It accompanies this paper at: https://doi.org/10.48130/ebp-0025-0006.

Author contributions

The authors confirm their contributions to the paper as follows: study conception and design: Li S, Chen Y, Wu M, Zhang P, Cui P, Duan W, Pan B, Xing B; material preparation, data collection and analysis: Li S, Chen Y; writing – draft manuscript preparation: Li S, Pan B, Chen Y; writing – review & editing: Pan B, Xing B, Wu M, Cui P, Zhang P, Duan W. All authors commented on previous versions of the manuscript. All authors reviewed the results and approved the final version of the manuscript.

Data availability

The datasets generated during and/or analyzed in the current study are available from the corresponding author on reasonable request.

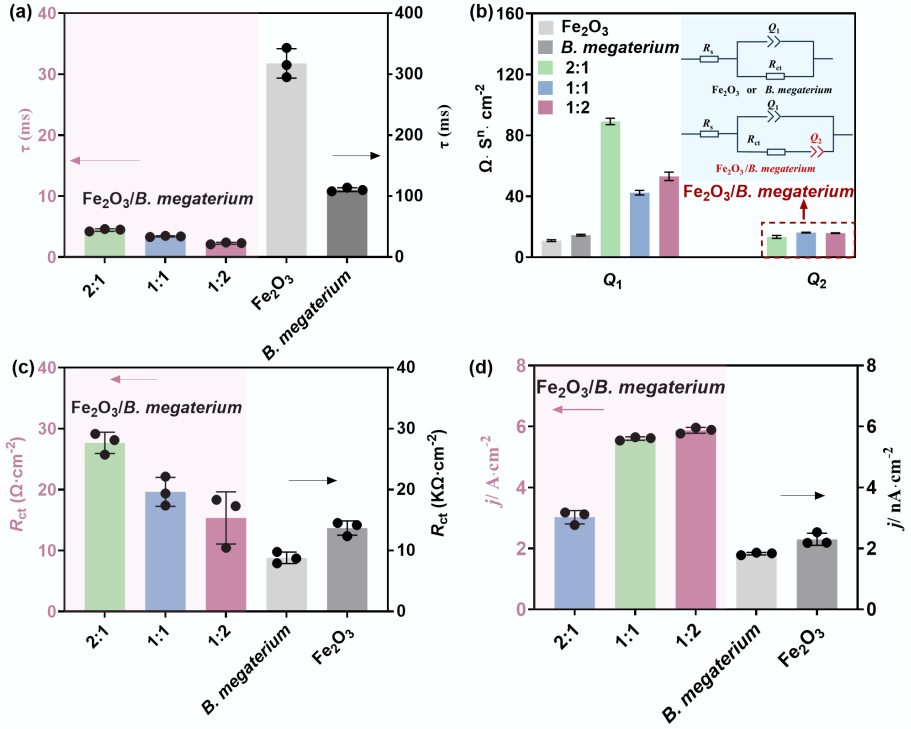

Fig. 4 The Fe_2O_3/*B. megaterium* biofilm is conducive to electron transfer. (**a**) Time constant τ values of the composites were significantly lower than that of Fe_2O_3 or *B. megaterium* under light. (**b**) The interface double-layer capacitance Q_1 of the composite system increased by 5 to 9 times compared to the individual system, and a new pseudo-capacitance Q_2 was formed. (**c**) The R_{ct} of Fe_2O_3/*B. megaterium* composites decreased by approximately three orders of magnitude compared to that of Fe_2O_3 or *B. megaterium* alone. (**d**) The exchange current density j of biofilm surpasses that of Fe_2O_3. The results of FeOOH and *B. megaterium* are presented in Supplementary Table S2.

Funding

This work was supported by the National Natural Science Foundation of China (42130711, 42377250, and 42267003), the National Key Research and Development Program of China (2023YFC3709100), the Yunnan Major Scientific and Technological Projects (202202AG050019), the Yunnan Fundamental Research Projects (202301AU070078, 202201BE070001-040), and Guided by the Central Government for Local Science and Technology Development Funds (202407AB11026).

Declarations

Competing interests

The authors declare that they have no conflict of interest.

Author details

[1]Yunnan Provincial Key Laboratory of Soil Carbon Sequestration and Pollution Control, Faculty of Environmental Science & Engineering, Kunming University of Science & Technology, Kunming 650500, China; [2]Yunnan International Joint Laboratory for Emission Reduction and Carbon Sequestration in Agricultural Soils, Kunming 650500, Yunnan, China; [3]Stockbridge School of Agriculture, University of Massachusetts, Amherst, MA 01003, USA

References

[1] Wild M, Gilgen H, Roesch A, Ohmura A, Long CN, et al. 2005. From dimming to brightening: decadal changes in solar radiation at Earth's surface. *Science* 308:847–850

[2] Gunina A, Kuzyakov Y. 2022. From energy to (soil organic) matter. *Global Change Biology* 28:2169–2182

[3] Lu A, Li Y, Ding H, Xu X, Li Y, et al. 2019. Photoelectric conversion on Earth's surface via widespread Fe- and Mn-mineral coatings. *Proceedings of the National Academy of Sciences* 116:9741–9746

[4] Huang S, Chen K, Chen X, Liao H, Zeng RJ, et al. 2023. Sunlight significantly enhances soil denitrification via an interfacial biophotoelectrochemical pathway. *Environmental Science and Technology* 57:7733–7742

[5] Claassens NJ, Sousa DZ, dos Santos VAPM, de Vos WM, van der Oost J. 2016. Harnessing the power of microbial autotrophy. *Nature Reviews Microbiology* 14:692–706

[6] Lu A, Li Y, Jin S, Wang X, Wu XL, et al. 2012. Growth of non-phototrophic microorganisms using solar energy through mineral photocatalysis. *Nature Communications* 3:768

[7] Chen S, Chen J, Zhang L, Huang S, Liu X, et al. 2023. Biophotoelectrochemical process co-driven by dead microalgae and live bacteria. *The ISME Journal* 17:712–719

[8] Dong H, Huang L, Zhao L, Zeng Q, Liu X, et al. 2022. A critical review of mineral–microbe interaction and co-evolution: mechanisms and applications. *National Science Review* 9:nwac128

[9] Li S, Wen X, Liu C, Dai Y, Shi X, et al. 2021. A sustainable way to reuse Cr(VI) into an efficient biological nanometer electrocatalyst by Bacillus megaterium. *Journal of Hazardous Materials* 409:124942

[10] Gao B, Sun M, Ding W, Ding Z, Liu W. 2021. Decoration of γ-graphyne on TiO_2 nanotube arrays: Improved photoelectrochemical and photoelectrocatalytic properties. *Applied Catalysis B: Environmental* 281:119492

[11] Li S, Li L, Wen X, Yang X, Shi X, et al. 2021. Ultrasmall Pd and PtPd nanoparticles for highly efficient catalysis directed by predesigned Morchella-inspired encapsulation. *Journal of Colloid and Interface Science* 585:368–375

[12] Guo J, Shi H, Huang X, Shi H, An Z. 2018. $AgCl/Ag_3PO_4$: A stable Ag-Based nanocomposite photocatalyst with enhanced photocatalytic activity for the degradation of parabens. *Journal of Colloid and Interface Science* 515:10–17
[13] Gao Y, Chen Y, Zhu F, Pan D, Huang J, et al. 2024. Revealing the biological significance of multiple metabolic pathways of chloramphenicol by *Sphingobium* sp. WTD-1. *Journal of Hazardous Materials* 469:134069
[14] Telkhozhayeva M, Hirsch B, Konar R, Teblum E, Lavi R, et al. 2022. 2D TiS_2 flakes for tetracycline hydrochloride photodegradation under solar light. *Applied Catalysis B: Environmental* 318:121872
[15] Tabelin CB, Corpuz RD, Igarashi T, Villacorte-Tabelin M, Alorro RD, et al. 2020. Acid mine drainage formation and arsenic mobility under strongly acidic conditions: Importance of soluble phases, iron oxyhydroxides/oxides and nature of oxidation layer on pyrite. *Journal of Hazardous Materials* 399:122844
[16] Zhou Y, Gao Y, Xie Q, Wang J, Yue Z, et al. 2019. Reduction and transformation of nanomagnetite and nanomaghemite by a sulfate-reducing bacterium. *Geochimica et Cosmochimica Acta* 256:66–81
[17] Ju W, Bagger A, Hao GP, Varela AS, Sinev I, et al. 2017. Understanding activity and selectivity of metal-nitrogen-doped carbon catalysts for electrochemical reduction of CO_2. *Nature Communications* 8:944
[18] Latthe S, Chougala N, Dodamani S, Badiger H, Kumbar S, et al. 2025. Electrochemical supercapacitor properties of CuO-doped α-Fe_2O_3 nanosheets under mT magnetic field. *Journal of Alloys and Compounds* 1010:177896
[19] Dong Y, Sanford RA, Boyanov MI, Flynn TM, O'Loughlin EJ, et al. 2020. Controls on iron reduction and biomineralization over broad environmental conditions as suggested by the firmicutes *Orenia metallireducens* Strain Z6. *Environmental Science & Technology* 54:10128–10140
[20] Panigrahi K, Mal S, Bhattacharyya S. 2024. Deciphering interfacial charge transfer mechanisms in electrochemical energy systems through impedance spectroscopy. *Journal of Materials Chemistry A* 12:14334–14353
[21] Li S, Wang X, Qin W, Wu M, Pan B, et al. 2025. Increased removal of ginsenoside Rb1 through the application of capacitance-enhanced biochars in soils. *Carbon Research* 4:32
[22] Qiao M, Wu Q, Wang Y, Gao S, Qin R, et al. 2024. Selective hydrogenation catalysis enabled by nanoscale galvanic reactions. *Chem* 10:3385–3395
[23] An N, Zhou L, Li W, Yuan X, Zhao L, et al. 2022. Multifunctional polymer coating cooperated with γ-Fe_2O_3 for boosting photoelectrochemical water oxidation. *Applied Catalysis B: Environmental* 318:121869